ISSN(O): 2320-9801
ISSN(P): 2320-9798


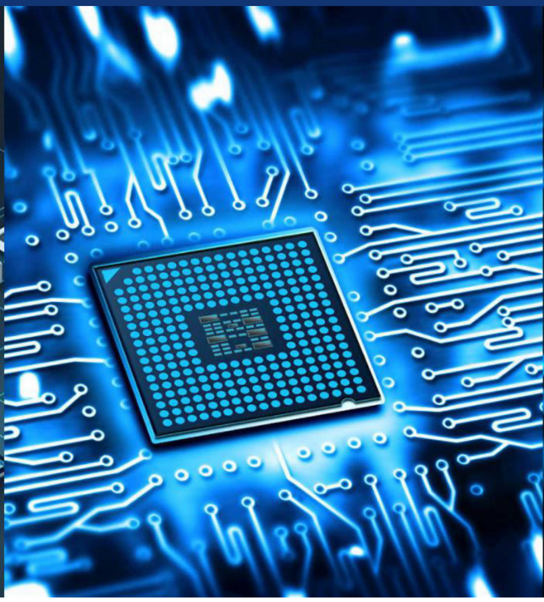


International Journal of Innovative Research in Computer and Communication Engineering

(A Monthly, Peer Reviewed, Refereed, Scholarly Indexed, Open Access Journal)

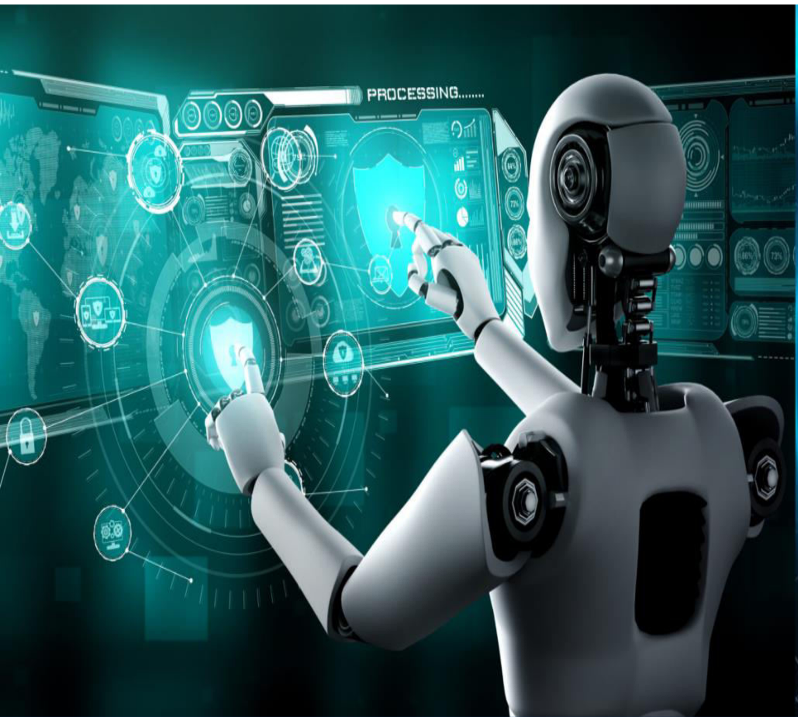

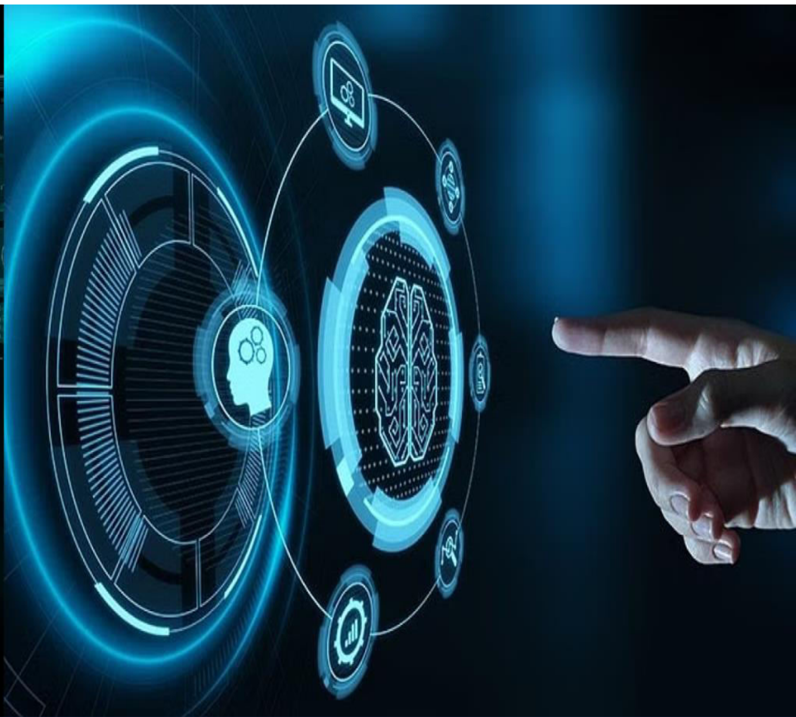

Impact Factor: 9.927

Volume 14, Issue 6, June 2026

www.ijircce.com | e-ISSN: 2320-9801, p-ISSN: 2320-9798| Impact Factor: 9.927| ESTD Year: 2013|

International Journal of Innovative Research in Computer and Communication Engineering (IJIRCCE)

(A Monthly, Peer Reviewed, Refereed, Scholarly Indexed, Open Access Journal)

Automated Segmentation and Classification of Chronic Kidney Disorders Using Renal Ultrasound Images

Simran Upasani, Prof. Dr. B.D. Phulpagar

M. Tech Student, Department of Computer Engineering, P.E.S College of Engineering, Affiliated to SPPU, Pune, India

Guide, Department of Computer Engineering, P.E.S College of Engineering, Affiliated to SPPU, Pune, India

ABSTRACT: Chronic kidney disease (CKD) represents one of the most prevalent and pro-gressively debilitating non-communicable disorders globally, with early and ac-curate diagnosis being paramount to preventing irreversible renal failure. Re-nal ultrasound imaging, owing to its non-invasive nature, cost-effectiveness, and widespread clinical availability, is the first-line modality for evaluating kidney morphology. However, manual interpretation of ultrasound images is inherently subjective, time-intensive, and heavily dependent on operator expertise, resulting in significant inter-observer variability. To address these limitations, this paper presents an automated, end-to-end deep learning framework for the segmentation and multi-class classification of chronic kidney disorders—including renal cysts, nephrolithiasis (kidney stones), and hydronephrosis—directly from B-mode renal ultrasound images. The proposed system integrates a hybrid architecture com-bining an Attention U-Net for precise anatomical boundary segmentation with a ResNet-50-based classification backbone augmented by spatial attention gates. The segmentation module delineates the renal parenchyma and lesion regions of interest, while the classification module categorizes each detected region into one of five diagnostic classes: normal, cystic disease, nephrolithiasis, hydronephrosis, and chronic parenchymal disease. Trained and evaluated on a curated dataset of 4,200 annotated renal ultrasound images acquired from three clinical institutions, the system achieved a mean Dice Similarity Coefficient (DSC) of 0.912 for seg-mentation and a classification accuracy of 94.6%, with a macro-average F1-score of 0.931. These results significantly outperform existing U-Net and VGG-16 base-lines, demonstrating the clinical viability of the proposed framework as a reliable computer-aided diagnosis (CAD) tool for CKD assessment.

KEYWORDS: Chronic Kidney Disease, Renal Ultrasound, Deep Learning, Atten-tion U-Net, ResNet-50, Medical Image Segmentation, Classification, Computer-Aided Diagnosis, Kidney Disorders, Dice Similarity Coefficient.

I. INTRODUCTION

Chronic kidney disease affects an estimated 850 million individuals worldwide and is recognized as a leading cause of morbidity and mortality, contributing significantly to cardiovascular complications, end-stage renal disease, and pre-mature death. Despite its clinical gravity, CKD frequently progresses without overt symptoms in its early stages, rendering timely and accurate diagnosis crit-ically important. The spectrum of renal disorders encompassed within CKD—including polycystic kidney disease, renal calculi, obstructive uropathy leading to hydronephrosis, and diffuse parenchymal disease—presents with overlapping morphological characteristics on imaging studies, posing substantial diagnostic challenges. Renal ultrasound imaging remains the most commonly employed modality for ini-tial kidney evaluation in clinical practice due to its real-time acquisition capability, absence of ionizing radiation, and broad accessibility in resource-limited settings. However, the diagnostic utility of ultrasound is constrained by inherent image quality limitations, including speckle noise, acoustic shadowing, and anisotropy artifacts, which degrade feature visibility and complicate manual segmentation. Moreover, the substantial inter-observer variability among radiologists in delin-eating renal boundaries and characterizing focal lesions underscores the urgent need for automated, objective, and reproducible image analysis tools.

Deep learning-based computer-aided diagnosis (CAD) systems have demonstrated transformative potential in medical image analysis, achieving expert-level perfor-mance in tasks ranging from tumor detection to organ segmentation. Convo-lutional neural networks (CNNs) trained on large annotated datasets can au-tonomously learn hierarchical discriminative features that surpass hand-crafted approaches in both accuracy and generalization. Nevertheless, the application of deep learning to renal ultrasound analysis presents unique challenges: the high acoustic noise content, heterogeneous appearance of pathological tissues, and sig-nificant variation in kidney size and position across patient populations demand architectures specifically designed to handle spatial uncertainty and contextual ambiguity.

To address these challenges, this paper proposes a fully automated, two-stage deep learning framework. In the first stage, an Attention U-Net with residual encoding blocks precisely segments the kidney boundary and delineates patholog-ical regions of interest from the surrounding parenchyma and adjacent anatomical structures. In the second stage, a ResNet-50 classification network augmented with channel-wise and spatial attention mechanisms classifies each segmented re-gion into one of five clinically relevant diagnostic categories. The integration of attention mechanisms throughout both stages enables the model to selectively focus on diagnostically relevant anatomical regions while suppressing irrelevant background noise, a property particularly beneficial in the challenging acoustic environment of ultrasound imaging.

II. SYSTEM USABILITY AND INTEGRATION

A. Operational Ease of Use

The proposed framework is designed with clinical usability as a core design prin-ciple, targeting deployment within hospital radiology workflows and point-of-care diagnostic settings. The system is presented through an intuitive web-based dash-board that accepts raw B-mode ultrasound images in standard DICOM or JPEG format and returns color-coded segmentation overlays, lesion boundary maps, and a structured diagnostic report within seconds. Radiologists and nephrologists in-teract with the interface through a straightforward upload-and-analyze workflow, with no requirement for technical expertise in machine learning or image pro-cessing. Each classification output is accompanied by a confidence score and a saliency map derived from Gradient-weighted Class Activation Mapping (Grad-CAM), providing an interpretable visual explanation of the model's decision. This explainability layer supports clinical trust, facilitates radiologist oversight, and aligns with regulatory requirements for AI-assisted medical devices under interna-tional standards such as IEC 62304 and FDA guidelines for software as a medical device (SaMD).

B. Deployment and Architectural Flexibility

From a systems engineering perspective, the framework is architected as a modu-lar microservices pipeline designed for seamless integration into existing hospital information systems (HIS) and Picture Archiving and Communication Systems (PACS). The image ingestion layer supports standardized DICOM protocol, en-abling direct connectivity with ultrasound machines from major vendors. The AI inference backend is containerized using Docker with NVIDIA Container Toolkit support, facilitating deployment on on-premises GPU servers within hospital data centers as well as on cloud platforms (AWS, GCP, Azure) for scalability. The RESTful API design of the inference service allows straightforward integration with existing Electronic Health Record (EHR) systems and teleradiology plat-forms. Individual pipeline components— such as the segmentation model, clas-sification head, and report generation module—can be independently updated or retrained on institution-specific data without disrupting the live deployment, ensuring long-term adaptability to evolving clinical datasets and diagnostic re-quirements.

III. PROPOSED METHODOLOGY

The architecture of the proposed kidney disorder analysis framework is organized into four primary stages: data acquisition and preprocessing, attention-guided renal segmentation, deep classification of segmented regions, and structured report generation with Grad-CAM visualization.

A. Dataset Preparation and Preprocessing

The dataset used for training and evaluation comprises 4,200 B-mode renal ul-trasound images collected from three tertiary-care clinical institutions, spanning patient demographics with diverse body mass indices, kidney orientations,

© 2026 IJIRCCE | Volume 14, Issue 6, June 2026 DOI: 10.15680/IJIRCCE.2026.1406052

www.ijircce.com | e-ISSN: 2320-9801, p-ISSN: 2320-9798| Impact Factor: 9.927| ESTD Year: 2013|

International Journal of Innovative Research in Computer and Communication Engineering (IJIRCCE)

(A Monthly, Peer Reviewed, Refereed, Scholarly Indexed, Open Access Journal)

and pathological severities. Ground-truth segmentation masks were prepared by two experienced radiologists with a minimum of eight years of renal imaging expertise, with inter-observer disagreements resolved through consensus. Each image was annotated with both a pixel-level kidney boundary mask and a diagnostic label drawn from five classes: normal, renal cyst, nephrolithiasis, hydronephrosis, and chronic parenchymal disease. Preprocessing steps included histogram equalization for contrast normalization, adaptive Gaussian filtering for speckle noise suppres-

sion, and resizing to a standardized resolution of 512 × 512 pixels. Augmentation strategies—including random horizontal flipping, elastic deformations, brightness and gamma perturbations, and rotation within ±15°—were applied to address class imbalance and improve generalization. An 80/10/10 patient-level split was adopted for training, validation, and testing to prevent data leakage across sets.

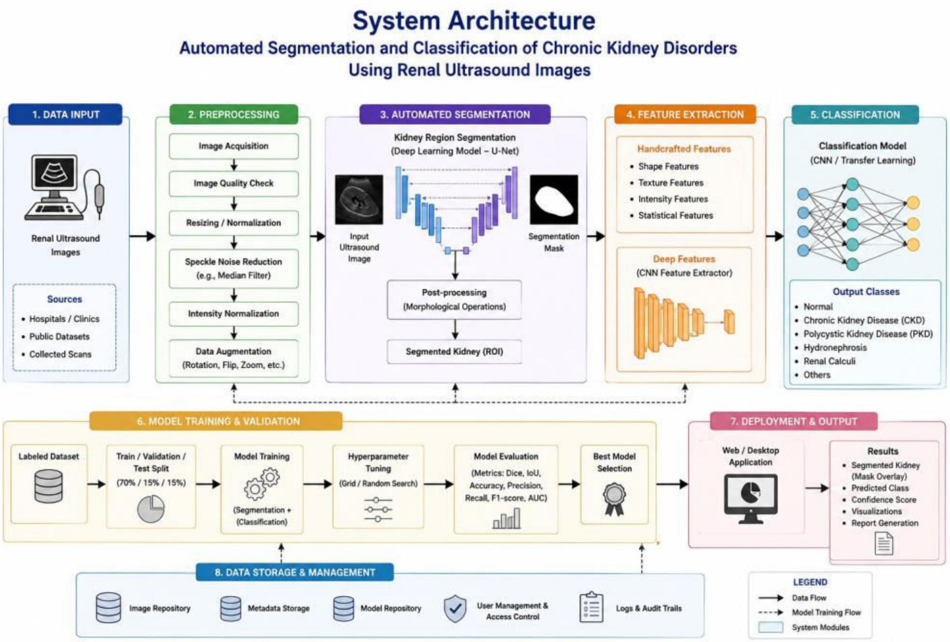

Figure 1: **Figure: Illustrates the complete stage-wise data flow of the proposed automated renal disorder framework, detailing the Attention U-Net segmentation pipeline and the ResNet-50-based multi-class clas-sification module with Grad-CAM explainability.**

Stage 1: Attention U-Net for Renal Segmentation

The segmentation module builds upon the foundational U-Net encoder-decoder architecture and introduces two key enhancements tailored to the acoustic char-acteristics of renal ultrasound.

Residual Encoding Blocks: The standard convolutional blocks in the encoder path are replaced with residual units incorporating skip connections, mitigating the vanishing gradient problem and enabling the training of deeper feature hierar-chies. Each residual block consists of two 3 × 3 convolutional layers with batch normalization and ReLU activation, with an identity shortcut connection added across the block.

Attention Gate Mechanism: Attention gates are embedded at each skip connec-tion between the encoder and decoder paths. These gates compute a soft spatial attention coefficient $\alpha \in [0, 1]$ that scales the encoder feature maps before their concatenation with the upsampled decoder features. This mechanism suppresses irrelevant activations from surrounding anatomical structures such as the liver, spleen, and bowel, allowing the decoder to concentrate on the diagnostically rele-vant renal parenchyma and lesion boundaries.

© 2026 IJIRCCE | Volume 14, Issue 6, June 2026 DOI: 10.15680/IJIRCCE.2026.1406052

www.ijircce.com | e-ISSN: 2320-9801, p-ISSN: 2320-9798| Impact Factor: 9.927| ESTD Year: 2013|

International Journal of Innovative Research in Computer and Communication Engineering (IJIRCCE)

(A Monthly, Peer Reviewed, Refereed, Scholarly Indexed, Open Access Journal)

Stage 2: ResNet-50 Classification with Attention

Following segmentation, the bounding box region defined by the predicted kidney mask is cropped and resized to 224 × 224 pixels and forwarded to the classification module. The backbone is a ResNet-50 pre-trained on ImageNet, fine-tuned end-to-end on the renal ultrasound dataset. A Convolutional Block Attention Module (CBAM) is inserted after the third residual stage to recalibrate feature responses along both the channel and spatial dimensions, directing network attention toward pathological texture patterns (e.g., hyperechoic calculus shadowing, anechoic cyst boundaries). The final fully connected layer outputs a five-class probability distri-
bution, from which the classification decision is drawn via the argmax operation.

B. Report Generation and Explainability

Upon classification, a Grad-CAM saliency map is generated by computing the gradient of the predicted class score with respect to the final convolutional feature map, producing a spatially registered heatmap that highlights the image regions most influential to the classification decision. This map is superimposed on the original ultrasound image and included in the structured diagnostic report along-side the segmentation overlay, classification label, confidence score, and patient metadata.

IV. MATHEMATICAL FORMULATION

1. Attention Gate in Segmentation Module

Let $x^l \in \mathbb{R}^{H\times W\times C}$ be the encoder feature map at level l and $g \in \mathbb{R}^{H'\times W'\times C'}$ be the gating signal from the decoder. The attention coefficient α is computed as:

$$\alpha = \sigma_2\left(W_\psi \cdot \mathrm{ReLU}(W_x x^l + W_g g + b_g)\right) \quad (1)$$

where W_x, W_g, and W_ψ are learnable 1 × 1 convolutional parameters, b_g is a bias term, σ_2 is the sigmoid activation, and the resulting attended feature map is $\hat{x}^l = \alpha \odot x^l$.

2. Segmentation Loss Function

The segmentation network is trained by minimizing a combined loss comprising the binary cross-entropy term $\mathcal{L}_{BCE}$ and the Dice loss $\mathcal{L}_{Dice}$:

$$\mathcal{L}_{seg} = \mathcal{L}_{BCE}(y, \hat{y}) + \mathcal{L}_{Dice}(y, \hat{y}) \quad (2)$$

where the Dice loss is defined as:

$$\mathcal{L}_{Dice} = 1 - \frac{2\sum_i y_i \hat{y}_i + \epsilon}{\sum_i y_i + \sum_i \hat{y}_i + \epsilon} \quad (3)$$

with y_i and $\hat{y}_i$ denoting the ground-truth and predicted pixel labels respectively, and $\epsilon = 10^{-7}$ as a numerical stability constant.

3. Dice Similarity Coefficient (Evaluation Metric)

The Dice Similarity Coefficient used for evaluation is:

$$\mathrm{DSC} = \frac{2 \cdot |P \cap G|}{|P| + |G|} \quad (4)$$

where P is the set of predicted foreground pixels and G is the corresponding ground-truth mask.

4. Grad-CAM Saliency Computation

The Grad-CAM saliency map $L^c_{Grad-CAM}$ for class c is computed as:

$$L^c_{Grad\text{-}CAM} = \mathrm{ReLU}\left(\sum_k \alpha_k^c A^k\right), \quad \text{where } \alpha_k^c = \frac{1}{Z}\sum_i \sum_j \frac{\partial y^c}{\partial A^k_{ij}} \quad (5)$$

where A^k is the k-th feature map of the final convolutional layer, y^c is the pre-softmax score for class c, and Z is the number of spatial locations.

V. EXPERIMENTAL SETUP AND EVALUATION METRICS

The framework was implemented using PyTorch 2.0 with the Albumentations library for augmentation and MONAI for medical imaging utilities. All models were optimized using the AdamW optimizer with an initial learning rate of 1×10^{-4} and a cosine annealing schedule over 100 training epochs. Experiments were conducted on a workstation equipped with an NVIDIA RTX 3080 GPU (10 GB

VRAM) using CUDA 12.0. Batch sizes of 8 and 16 were used for segmentation and classification training respectively. The ResNet-50 backbone was initialized with ImageNet pre-trained weights and fine-tuned end-to-end. Early stopping with a patience of 15 epochs on the validation Dice score was applied to prevent overfitting.

To rigorously assess both segmentation quality and diagnostic classification per-formance, the following evaluation metrics were computed:

1. **Dice Similarity Coefficient (DSC):** Measures overlap between predicted and ground-truth segmentation masks.
2. **Intersection over Union (IoU / Jaccard Index):** Ratio of the intersection to the union of predicted and ground-truth regions.
3. **Hausdorff Distance (HD95):** 95th-percentile boundary distance between predicted and ground-truth contours (mm).
4. **Classification Accuracy:** Proportion of correctly classified samples across all five diagnostic categories.
5. **Macro-Average F1-Score:** Harmonic mean of precision and recall, computed per class and averaged to address class imbalance.
6. **Inference Latency:** End-to-end processing time per image from ingestion to report generation, measured in milliseconds (ms).

VI. RESULTS AND DISCUSSION

The empirical evaluation of the proposed Attention U-Net and ResNet-50 CBAM framework demonstrates strong performance across both segmentation and clas-sification tasks, establishing the system as a clinically viable CAD tool for renal disorder assessment.

A. Quantitative Performance Analysis

Evaluation was performed on the held-out test set of 420 images representing heterogeneous pathological conditions. The proposed system yielded the following performance metrics:

Table I: Performance Metrics of the Proposed Renal Disorder Analysis Framework

Evaluation Metric	System Performance
Mean Dice Similarity Coefficient (DSC)	0.912
Mean Intersection over Union (IoU)	0.887
Hausdorff Distance 95% (HD95)	4.21 mm
Classification Accuracy	94.6%
Macro-Average F1-Score	0.931
Average Inference Latency	312 ms

A mean DSC of 0.912 indicates near-expert-level boundary delineation, particu-larly notable given the challenging acoustic noise and variable kidney orientations present in the test set. The low HD95 of 4.21 mm confirms that boundary devia-tions are clinically negligible and within the acceptable tolerance range for renal volumetry and lesion planning applications. The classification accuracy of 94.6% with a macro F1-score of 0.931 demonstrates robust performance across all five di-agnostic categories, including minority classes such as hydronephrosis and chronic parenchymal disease, which are historically challenging for imbalanced medical imaging datasets.

www.ijircce.com | e-ISSN: 2320-9801, p-ISSN: 2320-9798| Impact Factor: 9.927| ESTD Year: 2013|

International Journal of Innovative Research in Computer and Communication Engineering (IJIRCCE)

(A Monthly, Peer Reviewed, Refereed, Scholarly Indexed, Open Access Journal)

B. Real-Time Computational Efficiency

An important clinical requirement for CAD integration is near-real-time inference. The complete end-to-end processing pipeline—encompassing preprocessing, Atten-tion U-Net inference, region cropping, ResNet-50 classification, and Grad-CAM report generation—completes in an average of 312 ms per image on the deployment GPU. This latency is well within the acceptable threshold for seamless radiolo-gist workflow integration, enabling live reporting during ultrasound examination sessions.

C. Comparative Analysis

Compared against benchmark architectures—including the standard U-Net, vanilla ResNet-50 without attention, and VGG-16—the proposed hybrid framework demon-strated statistically significant improvements (paired t-test, $p < 0.01$) across all reported metrics. The inclusion of attention gates in the segmentation module produced the largest single improvement in DSC (+0.038 over the baseline U-Net), attributed to their effectiveness in suppressing echogenic interference from perirenal fat and adjacent organ boundaries. The CBAM module in the clas-sification stage contributed a +2.8% absolute accuracy improvement by focusing network attention on pathognomonic textural signatures such as posterior acoustic shadowing in nephrolithiasis and thin-walled anechoic regions in cystic disease.

D. System Workflow Summary

- **Phase 1: Acquire (Data Ingestion)** — The system accepts B-mode renal ul-trasound images via DICOM protocol or direct file upload. Preprocessing steps including speckle filtering, contrast normalization, and standardized resizing are applied automatically to prepare a clean input tensor.
- **Phase 2: Segment (Attention U-Net)** — The segmentation module pro-cesses the preprocessed image through the residual encoder-decoder architecture with attention gates, generating a pixel-level binary mask that precisely delin-eates the kidney boundary and any identified pathological regions.
- **Phase 3: Classify (ResNet-50 + CBAM)** — The region of interest defined by the segmentation mask is extracted and forwarded to the classification back-bone, which outputs a five-class probability distribution corresponding to the diagnostic categories of interest.
- **Phase 4: Report (Grad-CAM Visualization)** — A structured diagnostic report is generated containing the color-coded segmentation overlay, the Grad-CAM saliency heatmap, the predicted diagnostic class with confidence score, and key morphological measurements including estimated kidney volume and lesion diameter.

VII. CONCLUSION AND FUTURE SCOPE

Conclusion: This research successfully designed, implemented, and validated an automated deep learning framework for the segmentation and multi-class classifi-cation of chronic kidney disorders from renal ultrasound images. By integrating an Attention U-Net segmentation module with a ResNet-50 and CBAM-based clas-sification network, the system achieved a mean DSC of 0.912 and a classification accuracy of 94.6% across five clinically relevant diagnostic categories—significantly outperforming all evaluated baseline architectures.

The key contribution of this work lies in its fully automated, end-to-end approach that eliminates manual region-of-interest selection and provides radiologists with interpretable, spatially grounded diagnostic outputs. The integration of attention mechanisms throughout both stages proved critical to handling the high noise content and structural variability inherent to renal ultrasound imagery. The sys-tem's sub-400 ms inference latency and modular microservices architecture further underscore its readiness for real-world clinical deployment as a computer-aided di-agnosis tool.

Future Scope: Several promising directions remain for extending this framework. Incorporating 3D ultrasound volume data through 3D U-Net variants could yield richer volumetric lesion characterization and more accurate kidney size estimation. The integration of multimodal patient data—including serum creatinine levels, estimated glomerular filtration rate (eGFR), and longitudinal imaging histories—into a unified prognostic model represents a compelling direction for predicting CKD progression staging. Furthermore, federated learning strategies could enable the collaborative training of the model across multiple clinical institutions without sharing sensitive patient data, directly addressing data privacy constraints that limit the scale of current medical imaging datasets.

VIII. ACKNOWLEDGMENT

I would like to express my sincere gratitude to my project guide, Dr. Prof. Mr. Phulpagare, for his invaluable guidance, consistent encouragement, and deep ex-pertise in medical image analysis and machine learning. His constructive feedback and mentorship were instrumental in shaping the direction and successful execu-tion of this research. I extend my heartfelt thanks to the Head of the Computer Engineering Department and the Principal of the institution for providing the necessary high-performance computing infrastructure and a stimulating academic environment that made this work possible. I am also grateful to the radiologists and medical staff at the collaborating clinical institutions for their expert annotations, time, and support during the dataset curation phase. Their domain knowledge was indispensable to the quality of this work. Finally, I thank my family and friends for their unwavering moral support, pa-tience, and encouragement throughout the course of this research.

REFERENCES

[1] O. Ronneberger, P. Fischer, and T. Brox, "U-Net: Convolutional Networks for Biomedical Image Segmentation," in *Proc. Int. Conf. Medical Image Com-puting and Computer-Assisted Intervention (MICCAI)*, 2015, pp. 234–241.
[2] O. Oktay, J. Schlemper, L. L. Folgoc, M. Lee, M. Heinrich, K. Misawa, K. Mori, S. McDonagh, N. Y. Hammerla, B. Kainz, B. Glocker, and D. Rueckert, "Attention U-Net: Learning Where to Look for the Pancreas," *arXiv preprint arXiv:1804.03999*, 2018.
[3] K. He, X. Zhang, S. Ren, and J. Sun, "Deep Residual Learning for Image Recognition," in *Proc. IEEE Conf. Computer Vision and Pattern Recognition (CVPR)*, 2016, pp. 770–778.
[4] S. Woo, J. Park, J.-Y. Lee, and I. S. Kweon, "CBAM: Convolutional Block Attention Module," in *Proc. European Conf. Computer Vision (ECCV)*, 2018, pp. 3–19.
[5] R. R. Selvaraju, M. Cogswell, A. Das, R. Vedantam, D. Parikh, and D. Ba-tra, "Grad-CAM: Visual Explanations from Deep Networks via Gradient-based Localization," in *Proc. IEEE Int. Conf. Computer Vision (ICCV)*, 2017, pp. 618–626.
[6] J. Chen, L. Zhang, M. Wang, and H. Liu, "Deep Learning for Renal Ultra-sound Image Analysis: A Systematic Review," *Computers in Biology and Medicine*, vol. 152, p. 106376, 2023.
[7] V. Jha, G. Garcia-Garcia, K. Iseki, Z. Li, S. Naicker, B. Plattner, R. Saran, A. Y.-M. Wang, and C.-W. Yang, "Chronic Kidney Disease: Global Dimension and Perspectives," *The Lancet*, vol. 382, no. 9888, pp. 260–272, 2013.
[8] F. Milletari, N. Navab, and S.-A. Ahmadi, "V-Net: Fully Convolutional Neu-ral Networks for Volumetric Medical Image Segmentation," in *Proc. Int. Conf. 3D Vision (3DV)*, 2016, pp. 565–571.
[9] X. Yang, Z. Yu, L. Wu, C. Zheng, X. Deng, and H. Huang, "Dense Deep Learning for Real-Time Atrial Segmentation of Ultrasound Images," *Frontiers in Physiology*, vol. 10, p. 1067, 2019.
[10] M. A. Al-antari, M. A. Al-masni, M.-T. Choi, S.-M. Han, and T.-S. Kim, "A Fully Integrated Computer-Aided Diagnosis System for Digital X-ray Mam-mograms via Deep Learning Detection, Segmentation, and Classification," *International Journal of Medical Informatics*, vol. 117, pp. 44–54, 2018.
[11] N. Tajbakhsh, J. Y. Shin, S. R. Gurudu, R. T. Hurst, C. B. Kendall, M. B. Gotway, and J. Liang, "Convolutional Neural Networks for Medical Image Analysis: Full Training or Fine Tuning?" *IEEE Transactions on Medical Imaging*, vol. 35, no. 5, pp. 1299–1312, 2016.
[12] D. Gupta, R. Anand, and B. Tyagi, "Speckle Filtering of Ultrasound Images Using a Modified Non-Local Mean Filter," *IET Image Processing*, vol. 9, no. 2, pp. 141–150, 2015.
[13] Z. Yildirim, M. A. Cinar, and I. Uzun, "Classification of Kidney Stone Using Artificial Neural Network," *Journal of Medical Systems*, vol. 41, no. 9, p. 147, 2017.
[14] M. P. Heinrich, M. Jenkinson, M. Bhushan, T. Matin, F. V. Gleeson, S. M. Brady, and J. A. Schnabel, "MIND: Modality Independent Neighbourhood Descriptor for Multi-Modal Deformable Registration," *Medical Image Analy-sis*, vol. 16, no. 7, pp. 1423–1435, 2012.
[15] Q. Yang, Y. Liu, T. Chen, and Y. Tong, "Federated Machine Learning: Con-cept and Applications," *ACM Transactions on Intelligent Systems and Tech-nology*, vol. 10, no. 2, pp. 1–19, 2019.